# The Modified Gamma Size Distribution Applied to Inhomogeneous and Nonspherical Particles: Key Relationships and Conversions

GRANT W. PETTY AND WEI HUANG

*University of Wisconsin—Madison, Madison, Wisconsin*

(Manuscript received 12 August 2010, in final form 5 February 2011)

ABSTRACT

The four-parameter modified gamma distribution (MGD) is the most general mathematically convenient model for size distributions of particle types ranging from aerosols and cloud droplets or ice particles to liquid and frozen precipitation. The common three-parameter gamma distribution, the exponential distribution (e.g., Marshall–Palmer), and power-law distribution (e.g., Junge) are all special cases. Depending on the context, the particle ''size'' used in a given formulation may be the actual geometric diameter, the volume- or area-equivalent spherical diameter, the actual or equivalent radius, the projected or surface area, or the mass.

For microphysical and radiative transfer calculations, it is often necessary to convert from one size representation to another, especially when comparing or utilizing distribution parameters obtained from a variety of sources. Furthermore, when the mass scales with $D^b$, with $b < 3$, as is typical for snow and ice and other particles having a quasi-fractal structure, an exponential or gamma distribution expressed in terms of one size parameter becomes an MGD when expressed in terms of another. The MGD model is therefore more fundamentally relevant to size distributions of nonspherical particles than is often appreciated.

The central purpose of this paper is to serve as a concise single-source reference for the mathematical properties of, and conversions between, atmospheric particle size distributions that can expressed as MGDs, including exponential and gamma distributions as special cases.

For illustrative purposes, snow particle size distributions published by Sekhon and Srivastava, Braham, and Field et al. are converted to a common representation and directly compared for identical snow water content, allowing large differences in their properties to be discerned and quantified in a way that is not as easily achieved without such conversion.



## 1. Introduction

Among the most commonly used and mathematically convenient models for atmospheric particle size distributions (PSDs), ranging from aerosols and cloud droplets to liquid and frozen precipitation, are those encompassed by the four-parameter modified gamma distribution (Deirmendjian 1969), which has the generic form

$$n(x) = N_0 x^{\mu} \exp(-\Lambda x^{\gamma}). \quad (1)$$

The three-parameter variant, usually known simply as the gamma distribution, is obtained by setting $\gamma = 1$. The two-parameter exponential distribution and power-law distribution are obtained, respectively, by further setting $\mu = 0$ or $\Lambda = 0$.

The exponential distribution and the three-parameter gamma distribution have long dominated the literature on rain and snow PSDs (Marshall and Palmer 1948; Sekhon and Srivastava 1970, hereafter SS70; Hansen and Travis 1974; Ulbrich 1983). The power-law distribution has often been used as a first-order representation of aerosol PSDs, starting with Junge (1955).

The full four-parameter modified (or generalized) gamma distribution (hereafter simply MGD) is used less frequently and is most often encountered in descriptions of haze, fog, and cloud droplet PSDs (Deirmendjian 1969; Tomasi et al. 1975; Hess et al. 1998; Vivekanandan et al. 1999). A major premise of this paper is that the MGD is more fundamentally relevant to theoretical and observational PSD work, especially with respect to inhomogeneous or irregular solid particles such as snow and cloud ice, than is often appreciated.

*Corresponding author address:* Grant W. Petty, Department of Atmospheric and Oceanic Science, University of Wisconsin—Madison, 1225 W. Dayton St., Madison, WI 53706.
E-mail: gpetty@aos.wisc.edu

DOI: 10.1175/2011JAS3645.1

Depending on the context, the preferred particle size descriptor used in a given PSD formulation may be the mass $m$, the actual geometric diameter $D_g$, the volume-equivalent (solid or liquid) spherical diameter $D_e$, the actual or volume-equivalent radius ($r_g$ or $r_e$), the projected area $A$, or the area-equivalent diameter $D_a$. For microphysical, chemical, and radiative transfer calculations, it is often necessary to convert from one representation to another, especially when comparing or utilizing distribution parameters obtained from a variety of sources.

While the derivation of these conversions is mathematically straightforward, it entails some effort and risk of error. This is especially true in the case of complex nonspherical particles for which $m$ is found to be proportional to $D^b$, with $b < 3$ (Locatelli and Hobbs 1974; Mitchell et al. 1996; Vivekanandan et al. 1999; Mitchell 2002; Heymsfield et al. 2002; Delanoë et al. 2007; Schmitt and Heymsfield 2010; Heymsfield et al. 2010), and the two-dimensional $A$ is proportional to $D^\beta$ with $\beta < 2$ (Mitchell 1996; Schmitt and Heymsfield 2010).

Noteworthy for the purposes of this paper is that for such particles, even a simple exponential distribution expressed in terms of $D_g$ becomes an MGD when expressed in terms of melted-equivalent diameter $D_e$, and vice versa. For example, if the particle mass is proportional to $D_g^2$ (representative of snowflakes) and the associated PSD is $n_g(D_g) = N_{0g}\exp(-\Lambda_g D_g)$, then the PSD for the melted-equivalent diameters is $n_e(D_e) = N_{0e}D_e^{1/2}\exp(-\Lambda D_g^{3/2})$, an MGD.

A major objective of this paper is to provide a single-source reference for the relationships and conversions most likely to be of interest to those working with atmospheric PSDs in the MGD family, especially when particles of nonconstant effective density are involved. Apart from their potential use in quantitative calculations, one practical benefit is the ability to transform published PSDs from different sources to a common basis for ease of comparison.

We begin by briefly reviewing the relevant terminology and key mathematical relationship, starting with generic PSDs (next section) and then focusing specifically on the MGD in section 3. In section 4 we discuss the implications of various choices for representing particle size, followed by a tabulation of general relationships for converting between these representations in section 5 and implications for estimating model parameters in section 6. In section 7 we briefly discuss the rescaling or normalizing of PSDs (Testud et al. 2001; Lee et al. 2004; Delanoë et al. 2005; Field et al. 2007, hereafter F07) in the specific context of MGDs. In section 8, we illustrate the use of the aforementioned conversions by directly comparing three PSD models (SS70; Braham 1990, hereafter B90; F07) published using incompatible representations of particle size.

## 2. General properties of size distributions

A particle size distribution $n(x)$, where $x$ is some nonnegative variable (e.g., mass or diameter) that uniquely characterizes a particle's size, is generally defined such that

$$n(x)\,dx = \begin{pmatrix}\text{number of particles per unit volume}\\ \text{of air whose size falls in the range}\\ [x, x+dx]\end{pmatrix}.$$

Given $n(x)$, one may immediately compute several aggregate or bulk quantities from the distribution. The total number concentration of particles of all sizes is

$$N_{\text{tot}} = \int_0^\infty n(x)\,dx. \quad (2)$$

All other aggregate properties of the distribution, such as total surface area, mass, radiative extinction, radar or lidar backscatter, etc., are obtained by supplying an expression $f(x)$ that describes the contribution by a single particle of size $x$ and then integrating over all sizes:

$$F = \int_0^\infty f(x)n(x)\,dx. \quad (3)$$

Rather commonly, the function $f(x)$ that describes the single-particle contribution to an aggregate property of a distribution can be adequately modeled, at least statistically if not deterministically, as a power law; that is,

$$f(x) = \xi x^\delta, \quad (4)$$

in which case the associated aggregate property can be obtained as

$$F = \xi\int_0^\infty x^\delta n(x)\,dx = \xi M_\delta, \quad (5)$$

where the $M_\delta$ is the $\delta$th moment of $n(x)$.

For any physically reasonable and therefore finite $f(x)$, the corresponding aggregate property $F$ must also be finite. This requirement restricts the set of admissible size distribution models $n(x)$. It is not difficult to construct hypothetical size distributions [e.g., $n(x) \propto 1/(1/x + x^4)$] for which low-order moments (e.g., total particle count) are well defined while higher-order moments (e.g., total particle volume) are infinite, or vice versa.

## 3. The modified gamma distribution

### a. Definition

What is now commonly known as MGD was apparently introduced to represent PSDs by Deirmendjian (1963). It is given by

$$n(x) = N_0 x^{\mu} \exp(-\Lambda x^{\gamma}). \tag{6}$$

It is therefore a four-parameter model for $n(x)$, with $\mu$, $\Lambda$, and $\gamma$ controlling the shape of the distribution and $N_0$ controlling the overall scaling. If $x$ has dimensions of length (the most common case), then $N_0$ has dimensions $L^{-(\mu+4)}$ and $\Lambda$ has dimensions $L^{-\gamma}$. Because of the dependence of the dimensions of $N_0$ and $\Lambda$ on the values of $\mu$ and $\gamma$, respectively, one cannot meaningfully compare values of the first two parameters for different distributions if $\mu$ and/or $\gamma$ differ as well.

Variations on the above form, all equivalent, have appeared in the literature. For example, Tomasi et al. (1975) and Muller et al. (1993) give the MGD (with adjusted notation) as

$$n(x) = N_0 x^{\mu} \exp\left[-\frac{\mu}{\gamma}\left(\frac{x}{x_0}\right)^{\gamma}\right], \tag{7}$$

where $x_0$ is the modal value of $x$.

Another equivalent form, given by Auf der Maur (2001) can be written (with some notational adjustments) as a probability distribution function (PDF):

$$p(x) = C\left(\frac{x}{c}\right)^{\gamma u-1} \exp\left[-\left(\frac{x}{c}\right)^{\gamma}\right], \tag{8}$$

where $C$ is a normalization constant that depends on distribution parameters $\gamma$, $c \equiv \Lambda^{1/\gamma}$, and $u \equiv (\mu + 1)/\gamma$, with the full PSD then given by $n(x) = N_{\mathrm{tot}} p(x)$.

Occasionally one encounters the term ''modified gamma distribution'' applied to a three-parameter gamma distribution (Schneider and Stephens 1995; Babb et al. 1999; Miles et al. 2000; Maki et al. 2001), but this usage does not appear to be widespread.

### b. Relationship to other models

#### 1) Exponential distribution

The MGD encompasses a number of common two- and three-parameter distributions as special cases. For example, by setting $\mu = 0$ and $\gamma = 1$, we obtain the widely used exponential distribution

$$n(x) = N_0 \exp(-\Lambda x), \tag{9}$$

of which perhaps the best-known example is the Marshall and Palmer (1948) model of the distribution of rain drop sizes. The general form has been adapted to snow aggregates by Gunn and Marshall (1958) and SS70, among many others.

#### 2) Power-law distribution

Similarly, a power-law distribution, as exemplified by the Junge (1955) model for aerosol sizes, is obtained by letting $\Lambda = 0$:

$$n(x) = N_0 x^{\mu}. \tag{10}$$

The moments of this distribution on the interval $[0, \infty]$ do not exist; therefore, a power-law distribution can only be physically meaningful for finite range $[x_{\min}, x_{\max}]$, in which case

$$M_k = \frac{N_0}{\mu + k + 1}\left(x_{\max}^{\mu+k+1} - x_{\min}^{\mu+k+1}\right). \tag{11}$$

The expressions presented below for various moments of MGDs are undefined for $\Lambda = 0$ and are in any case applicable only when $n(x)$ is continuous for all non-negative $x$. For this reason, we will not discuss power-law PSDs further in this paper, though the conversions given in section 5 may still be used.

#### 3) Gamma distribution

The more general three-parameter gamma distribution, which results from setting $\gamma = 1$, is in wide use for precipitation (Ulbrich 1983, 1985; Kozu and Nakamura 1991; Meneghini et al. 1992; Jameson 1993; Iguchi et al. 2000; Maki et al. 2001; Grecu et al. 2004; Rose and Chandrasekar 2006), as well as for cloud droplets and cirrus ice particles (Ackerman and Stephens 1987; Schneider and Stephens 1995; Mitchell et al. 1996; Babb et al. 1999; Miles et al. 2000; Mitchell 2002; Heymsfield et al. 2004; Sun et al. 2006):

$$n(x) = N_0 x^{\mu} \exp(-\Lambda x). \tag{12}$$

In exponential and gamma distributions, $N_0$ and $\Lambda$ are often known respectively as the intercept and slope parameters; $\mu$ is often referred to as the shape parameter.

A commonly used alternative formulation of (12) is given by Hansen and Travis (1974):

$$n(r) = N_0 r^{(1-3v_{\mathrm{eff}})/v_{\mathrm{eff}}} \exp\left(\frac{-r}{r_{\mathrm{eff}} v_{\mathrm{eff}}}\right), \tag{13}$$

where $r_{\mathrm{eff}}$ is the effective radius of the distribution, defined in this context[1] as

$$r_{\mathrm{eff}} \equiv \frac{\int_0^\infty r^3 n(r)\,dr}{\int_0^\infty r^2 n(r)\,dr} > 0, \tag{14}$$

and the effective variance is

$$v_{\mathrm{eff}} \equiv \frac{\int_0^\infty (r - r_{\mathrm{eff}})^2 r^2 n(r)\,dr}{r_{\mathrm{eff}}^2 \int_0^\infty r^2 n(r)\,dr} > 0. \tag{15}$$

For the three-parameter distribution, we thus have

$$\Lambda = \frac{1}{r_{\mathrm{eff}} v_{\mathrm{eff}}}; \quad \mu = \frac{1 - 3v_{\mathrm{eff}}}{v_{\mathrm{eff}}}. \tag{16}$$

For the special case that $\mu = 0$ (exponential PSD), it follows that $v_{\mathrm{eff}} = 1/3$ and $\Lambda = 3/r_{\mathrm{eff}}$.

#### 4) OTHER PSD MODELS

PSD models in occasional use that are not simply special cases of (6) include the normal distribution and the lognormal distribution. For example, Tian et al. (2010) found that some observed cirrus ice particle spectra are better fit by a lognormal distribution than by exponential or gamma distributions (they did not, however, investigate the fit by an MGD).

While many of the general considerations outlined in this paper are valid for lognormal distributions as well, the details of the mathematics require a separate treatment and will not be discussed in this paper. Some general properties of lognormal distributions are summarized by Straka (2009).

In addition, one sometimes encounters composite PSD models based on the sum of two simpler underlying PSDs. For example, Kuo et al. (2004) proposed a bimodal PSD model constructed from the sum of two MGDs. The moments of such a PSD are the sums of the moments of the individual MGDs. Other characteristics, such as the median mass particle size, cannot be derived analytically for a composite PSD.

Also, F07 published empirically derived size distributions for ice particles expressed as rescaled (nondimensional) size distributions $\Phi_{23}(x)$, where $x$ is a nondimensional (scaled) diameter. The fitted $\Phi_{23}(x)$ models are sums of pure exponentials and three-parameter gamma distributions with fixed parameters. We will return to the Field et al. PSD, as well as their rescaling procedure applied to an MGD, in sections 7 and 8.

[1] The conventional definition of "effective radius" is appropriate to spherical particles. See McFarquhar and Heymsfield (1998) for a variety of definitions applicable to nonspherical ice particles.

### c. *Moments and modes of the MGD*

#### 1) ANALYTIC EXPRESSIONS

Much of the usefulness of the MGD as a model for PSDs stems not only from its flexibility but from the existence of convenient analytical expressions for various properties of the distribution. In particular, the $k$th moment of the MGD is given by

$$M_k \equiv \int_0^\infty x^k n(x)\,dx = N_0 \int_0^\infty x^{k+\mu} \exp(-\Lambda x^\gamma)\,dx$$
$$= \frac{N_0}{\gamma} \frac{\Gamma\left(\frac{\mu + k + 1}{\gamma}\right)}{\Lambda^{(\mu+k+1)/\gamma}}, \tag{17}$$

where the gamma function $\Gamma(x)$ is the generalization of the integer factorial function $(x - 1)!$ to continuous $x$.

The total number of particles per unit volume is the zeroth moment of $n(x)$, or

$$N_{\mathrm{tot}} = \frac{N_0}{\gamma} \frac{\Gamma\left(\frac{\mu + 1}{\gamma}\right)}{\Lambda^{(\mu+1)/\gamma}}. \tag{18}$$

For $N_{\mathrm{tot}}$ to be finite, we require

$$\frac{\mu + 1}{\gamma} > 0. \tag{19}$$

Another characteristic of interest is the $k$th mode $x_k$ of the distribution, defined here as the value of $x$ coinciding with the maximum of the function $x^k n(x)$:

$$x_k = \left(\frac{\mu + k}{\Lambda\gamma}\right)^{1/\gamma}. \tag{20}$$

The mode of a size distribution is not an invariant property with respect to the choice of variable used to represent particle size except when the variables are linearly related.

A more comprehensive discussion of the analytic properties of modified gamma distributions is given by Straka (2009).

#### 2) PARAMETER ESTIMATION FROM REAL DATA

The analytical expressions for PSD moments given above depend on the MGD model being valid for all nonnegative $x$. When working with real data rather than models, it is often necessary to estimate moments and/or parameters of the PSD from observations that are only reliable within a restricted size range [$x_{\min}$, $x_{\max}$]. In general, parameter estimation from PSD observations is fraught with difficulties related to instrument limitations and statistical sampling, many aspects of which are discussed by Auf der Maur (2001), Smith and Kliche (2005), Brandes et al. (2007), Brawn and Upton (2007), Mallet and Barthes (2009), and Tian et al. (2010), among many others.

This paper does not attempt to address the problems associated with statistical sampling or truncation of observed spectra but rather focuses exclusively on the mathematical conversion between related MGDs, assuming that the parameters of the MGD are known. However, in section 6 we comment briefly on the potential for mathematical inconsistencies when fitting models to data.

### *d. Median mass particle size*

To conveniently communicate a gross property of a PSD, it is common to refer to the particle size that divides the total mass of the distribution into equal parts (Mitchell 1991). Generically, this median mass particle size $x_{\text{med}}$ is defined by the following relationship:

$$\int_0^{x_{\text{med}}} m(x)n(x)\,dx = \frac{W}{2} = \int_{x_{\text{med}}}^{\infty} m(x)n(x)\,dx, \quad (21)$$

where $m(x)$ is the particle mass, and the total mass concentration of the PSD is

$$W = \int_0^{\infty} m(x)n(x)\,dx. \quad (22)$$

Approximate analytic expressions for the median mass particle size in the case of an MGD will be given for the specific choices of size descriptor discussed in the following section.

## 4. Choice of size descriptor

In the previous sections, we used $x$ as a generic particle size without specifying its precise meaning. The choice of the size variable used in the mathematical representation of a PSD is very flexible, yet the choice affects both the values and the physical dimensions of the parameters $N_0$, $\mu$, $\Lambda$, and $\gamma$ in an MGD.

If one allows the term ''size'' to encompass all reasonable descriptions of how ''big'' a particle is, including mass or any of a number of possible measures of linear dimension, area, or volume, one finds that, in the case of irregular particles at least, only the particle mass has an unambiguous meaning that does not depend either on context or on arbitrary definitions. For example, is the ''diameter'' of a particle its absolute maximum dimension or rather that recorded by a 2D imaging probe? Is the particle ''volume'' defined as the volume of its circumscribing sphere or by some other measure of the spatial distribution of mass (Petty and Huang 2010)? (The definition of particle volume is of course also inseparable from the definition of particle density.)

Despite the potential ambiguities, there is not only no universal standard way to describe particle size but rather a number of distinct conventions, many in wide use, that lead to superficially incompatible descriptions of a PSD. One major purpose of the present paper is to summarize in convenient form the conversions from one size representation to another. A second purpose is to demonstrate that a simple exponential or gamma PSD referenced to one size descriptor (e.g., liquid equivalent spherical diameter) will often require representation by an MGD for almost any other choice of size descriptor (e.g., geometric diameter).

### *a. Mass m*

As noted above, the least ambiguous descriptor related to the size of any nonspherical or nonhomogeneous particle is $m$. Although it is not common to do so, we may elect to represent a PSD in terms of the distribution of particle masses. The four parameters of the MGD are supplied with subscripts to make clear their association with this variable, and the PSD thus takes the following form:

$$n_m(m) = N_{0m} m^{\mu_m} \exp(-\Lambda_m m^{\gamma_m}). \quad (23)$$

The total mass concentration represented by this distribution is then the first moment of this distribution:

$$W = \int_0^{\infty} m n_m(m)\,dm = \frac{N_{0m}}{\gamma_m} \frac{\Gamma\left(\frac{\mu_m + 2}{\gamma_m}\right)}{\Lambda_m^{(\mu_m+2)/\gamma_m}}. \quad (24)$$

Following (21), the median particle mass $m_{\text{med}}$ is then defined by the following relationship:

$$\int_0^{m_{\text{med}}} m n_m(m)\,dm = \frac{W}{2}. \quad (25)$$

The exact solution for $m_{\text{med}}$ must be expressed in terms of the incomplete gamma function $\gamma(a, x)$; however, a numerical representation of reasonable accuracy is

$$m_{\text{med}} = \left(\frac{\mu_m + 2 - 0.327\gamma_m}{\Lambda_m \gamma_m}\right)^{1/\gamma_m} \quad (26)$$

### b. Geometric diameter $D_g$

Considerably more variable in its meaning than the particle mass but generally easier to observe in the field is $D_g$ of the particle. One may then specify the size distribution as an MGD of the form

$$n_g(D_g) = N_{0g} D_g^{\mu_g} \exp(-\Lambda_g D_g^{\gamma_g}). \quad (27)$$

For nonspherical particles, the precise definition of $D_g$ is crucial. As a practical matter, it is often taken to be the maximum dimension of the particle as projected onto a two-dimensional image plane. For nonspherical randomly oriented particles, it is understood that this maximum dimension bears only a statistical relationship to the true maximum dimension of the particle itself. For example, in the worst-case scenario of a randomly oriented slender needle of length $L$, the projected maximum dimension $D_g$ obeys a rather broad PDF,

$$p(D_g) = \frac{\pi}{2L} \sin\left(\frac{\pi D_g}{2L}\right), \quad 0 \le D_g \le L, \quad (28)$$

with expectation value $\langle D_g \rangle \approx 0.64L$. Moreover, there may exist only a rough statistical relationship between the true maximum dimension of a stochastically aggregated snowflake, for example, and any other physical property of the aggregate, such as mass. Notwithstanding the likelihood of two layers of scatter in the relationship between observed $D_g$ and particle $m$, it is common to assume a power-law relationship between the two:

$$m = aD_g^b. \quad (29)$$

For the special case that the particles happen to be spherical and the density $\rho$ is independent of size, then we have $\alpha = \rho\pi/6$ and $b = 3$. More generally, however, it is often observed that density decreases with $D_g$, in which case $b < 3$ and $a > 0$ are empirically determined coefficients (Mitchell et al. 1996; Vivekanandan et al. 1999; Mitchell 2002; Heymsfield et al. 2002; Delanoë et al. 2007; Heymsfield et al. 2010).

Variable density implies a variable mixture of air and some solid material (e.g., ice) having fixed density $\rho_0$. If the fraction of solid material is $f$, and if we neglect the density of air, then $\rho = f\rho_0$. But because $f$ cannot exceed unity, there is a lower limit $D_{g,\min}$ to the size for which (29) can be valid when $b < 3$ (Brown and Francis 1995; Delanoë et al. 2007). In particular, if the particles are spherical, then

$$D_{g,\min} = \left(\frac{\pi\rho_0}{6a}\right)^{1/(b-3)}. \quad (30)$$

When evaluating integrals of a size distribution $n_g(D_g)$ for which $b < 3$, one should assess whether significant numerical errors might arise from assuming (30) for particles smaller than $D_{g,\min}$ (Heymsfield et al. 2010). If so, then numerical integration is in order. Otherwise, we may derive analytical expressions based on (17) to obtain bulk properties of the distribution. For example, the mass concentration is given by

$$W = \int_0^\infty aD_g^b n_g(D_g)\, dD_g = \frac{aN_{0g}}{\gamma_g} \frac{\Gamma\left(\frac{\mu_g + b + 1}{\gamma_g}\right)}{\Lambda_g^{(\mu_g+b+1)/\gamma_g}}. \quad (31)$$

Following (21), the median mass geometric diameter $D_{g,\text{med}}$ is defined by the relationship

$$\int_0^{D_{g,\text{med}}} aD_g^b n_g(D_g)\, dDg = \frac{W}{2}. \quad (32)$$

An approximate analytic expression is

$$D_{g,\text{med}} \approx \left(\frac{\mu_g + 1 + b - 0.327\gamma_g}{\Lambda_g \gamma_g}\right)^{1/\gamma_g}. \quad (33)$$

The above expression is a generalization of that given previously by Mitchell (1991) for a gamma distribution (i.e., $\gamma_g = 1$).

### c. Liquid- or solid-equivalent spherical diameter $D_e$

Sometimes it is convenient to express the size of a nonspherical or tenuous particle in terms of the diameter of a mass-equivalent homogeneous sphere of some standard density $\rho_0$. For example, the liquid-equivalent diameter of a snowflake is the diameter of the spherical water droplet that results from melting the snowflake.

The use of the equivalent spherical diameter $D_e$ is tantamount to taking $b = 3$ in (30) and $a$ equal to

$$a_0 \equiv \frac{\rho_0 \pi}{6}, \quad (34)$$

so that $D_e$ satisfies

$$m = a_0 D_e^3. \quad (35)$$

The MGD can be written in terms of $D_e$ as follows:

$$n_e(D_e) = N_{0e} D_e^{\mu_e} \exp(-\Lambda_e D_e^{\gamma_e}). \quad (36)$$

The mass concentration is

$$W = \int_0^\infty a_0 D_e^3 n_e(D_e)\, dD_e = \frac{a_0 N_{0e}}{\gamma_e} \frac{\Gamma\left(\frac{\mu_e + 4}{\gamma_e}\right)}{\Lambda_e^{(\mu_e+4)/\gamma_e}}. \quad (37)$$

The median mass equivalent diameter $D_{e,\mathrm{med}}$ is defined by the relationship

$$W = \int_0^{D_{e,\mathrm{med}}} a_0 D_e^3 n_e(D_e)\,dD_e = \frac{W}{2}. \quad (38)$$

An approximate analytic expression is

$$D_{e,\mathrm{med}} \approx \left(\frac{\mu_e + 4 - 0.327\gamma_e}{\Lambda_e \gamma_e}\right)^{1/\gamma_e}. \quad (39)$$

In the Rayleigh limit—that is, for water or ice particles much smaller than the radar wavelength—the radar backscatter cross section per unit volume distribution is approximately proportional to the radar reflectivity factor $Z$, which is defined as the sixth moment of the distribution of liquid-equivalent diameters:

$$Z = \int_0^\infty D_e^6 n_e(D_e)\,dD_e = \frac{N_{0e}}{\gamma_e} \frac{\Gamma\left(\frac{\mu_e + 7}{\gamma_e}\right)}{\Lambda_e^{(\mu_e+7)/\gamma_e}}. \quad (40)$$

### d. Area A and area-equivalent diameter $D_a$

In many areas of research, some convenient measure of a particle's projected area may be of primary interest, not only because it can be directly observed in the field, but also because of its relevance for radiative transfer, microphysical growth processes, and/or particle fall speeds (Mitchell and Arnott 1994; Mitchell 1996; Heymsfield and Miloshevich 2003; Mitchell and Heymsfield 2005). The projected area in question may either be that of a randomly oriented particle or else that of a particle that has a predictable alignment with respect to either an optical instrument or the direction of fall. For atmospheric chemical processes, as well as some radiative properties, it may be the total surface area of the particles rather than the projected area that matters. For fractal-like particles, any value given for either the surface area or projected area is almost certainly resolution dependent.

Notwithstanding the numerous variations, and subject to the same statistical caveats as for (29), we assume a power-law relationship between the geometric diameter and some measure of the particle's area:

$$A = \alpha D_g^\beta \quad (41)$$

If $A$ is the projected area and the particle is a sphere or circular disk oriented perpendicular to the line of sight, then $\alpha = \pi/4$ and $\beta = 2$. But for an irregular or fractal particle, typically $\alpha < \pi/4$ and/or $\beta < 2$ (Mitchell 1996; Schmitt and Heymsfield 2010).

Another descriptor based on the projected area $A$ is the so-called area ratio $A_r$ (Heymsfield and Miloshevich 2003; Schmitt and Heymsfield 2009), defined as

$$A_r \equiv \frac{4A}{\pi D_g^2} \quad (42)$$

and parameterized as

$$A_r = c_0 D_g^{c_1}. \quad (43)$$

The coefficients appearing in (41) and (43) are related as follows:

$$\alpha = \frac{\pi}{4} c_0, \quad \beta = c_1 + 2. \quad (44)$$

In the remainder of this paper, we use $\alpha$ and $\beta$ to characterize the area–diameter relationship.

If $A$ is instead taken to be the total surface area of the particle, then for a uniform sphere, $\alpha = \pi$ and $\beta = 2$. Nonspherical or irregular particles may have surface areas that are either larger or smaller than those of spheres having the same $D_g$, so there are few obvious constraints on possible values for $\alpha$ or $\beta$.

Regardless of the context-specific meaning of $A$, one may choose to define a size distribution in terms of $A$, in which case the MGD form is

$$n_A(A) = N_{0A} A^{\mu_A} \exp(-\Lambda_A A^{\gamma_A}). \quad (45)$$

One reason why this form might be of interest is that the parameters of the distribution, along with those of $n_g(D)$, can be directly estimated from 2D images of the particles without the need for ancillary assumptions.

Given the projected $A$ of a particle, one may also define $D_a$ such that

$$A = \alpha_0 D_a^2. \quad (46)$$

where

$$\alpha_0 \equiv \frac{\pi}{4}. \quad (47)$$

If instead $A$ represents total surface area, then a preferable choice might be $\alpha_0 = \pi$. Either way, we have the possibility for yet another PSD model,

$$n_a(D_a) = N_{0a} D_a^{\mu_a} \exp(-\Lambda_a D_a^{\gamma_a}). \quad (48)$$

### e. Radius

Sometimes dimensions are given in terms of the radius $r$ rather than the diameter $D$. Regardless of whether it is

TABLE 1. Complete set of conversions from one size descriptor (column heading) to another (row heading). Expressions in boldface are definitional; all others follow from these.

| | Conversion from | | | | |
|---|---|---|---|---|---|
| Conversion to | $m$ | $D_g$ | $D_e$ | $D_a$ | $A$ |
| $m$ | — | $\boldsymbol{aD_g^b}$ | $\boldsymbol{a_0D_e^3}$ | $a\left(\frac{\alpha_0}{\alpha}\right)^{b/\beta}D_a^{2b/\beta}$ | $a\left(\frac{A}{\alpha}\right)^{b/\beta}$ |
| $D_g$ | $\left(\frac{m}{a}\right)^{1/b}$ | — | $\left(\frac{a_0}{a}\right)^{1/b}D_e^{3/b}$ | $\left(\frac{\alpha_0}{\alpha}\right)^{1/\beta}D_a^{2/\beta}$ | $\left(\frac{A}{\alpha}\right)^{1/\beta}$ |
| $D_e$ | $\left(\frac{m}{a_0}\right)^{1/3}$ | $\left(\frac{a}{a_0}\right)^{1/3}D_g^{b/3}$ | — | $\left(\frac{a}{a_0}\right)^{1/3}\left(\frac{\alpha_0}{\alpha}\right)^{b/3\beta}D_a^{2b/3\beta}$ | $\left(\frac{a}{a_0}\right)^{1/3}\left(\frac{A}{\alpha}\right)^{b/3\beta}$ |
| $D_a$ | $\left(\frac{\alpha}{\alpha_0}\right)^{1/2}\left(\frac{m}{a}\right)^{\beta/2b}$ | $\left(\frac{\alpha}{\alpha_0}\right)^{1/2}D_g^{\beta/2}$ | $\left(\frac{a_0}{a}\right)^{\beta/2b}\left(\frac{\alpha}{\alpha_0}\right)^{1/2}D_e^{3\beta/2b}$ | — | $\left(\frac{A}{\alpha_0}\right)^{1/2}$ |
| $A$ | $\alpha\left(\frac{m}{a}\right)^{\beta/b}$ | $\boldsymbol{\alpha D_g^\beta}$ | $\alpha\left(\frac{a_0}{a}\right)^{\beta/b}D_e^{3\beta/b}$ | $\boldsymbol{\alpha_0D_a^2}$ | — |

the geometric or equivalent diameter and radius we are speaking of, we require

$$n(D)\,dD = n(2r)(2dr), \tag{49}$$

in which case

$$\begin{aligned} n(D)\,dD &= N_{0d}D^{\mu_d}\exp(-\Lambda_d D^{\gamma_d}) \\ &= 2N_{0d}(2r)^{\mu_d}\exp[-\Lambda_d(2r)^{\gamma_d}]\,dr, \end{aligned} \tag{50}$$

and

$$N_{0r} = 2^{\mu_d+1}N_{0d}, \quad \mu_r = \mu_d, \quad \gamma_r = \gamma_d, \quad \Lambda_r = 2^{\gamma_d}\Lambda_d. \tag{51}$$

## 5. Conversion between representations

If a PSD expressed in terms of size descriptor $x$ is to be transformed into PSD expressed in terms of size descriptor $y$, then we require

$$n_x(x)\,dx = n_x[x(y)]\frac{dx}{dy}\,dy = n_y(y)\,dy, \tag{52}$$

so that the conversion is obtained via

$$n_y(y) = n_x[x(y)]\frac{dx}{dy}. \tag{53}$$

For the MGD, we have that

$$N_{0y}y^{\mu_y}\exp(-\Lambda_y y^{\gamma_y}) = N_{0x}[x(y)]^{\mu_x}\exp\{-\Lambda_x[x(y)]^{\gamma_x}\}\frac{dx}{dy}. \tag{54}$$

For the case that $x$ and $y$ are related by a power law, then substituting appropriate expressions for $x(y)$ and its derivative into the above allows one to solve for the new parameters $N_{0y}$, $\mu_y$, $\Lambda_y$, and $\gamma_y$ in terms of the old parameters $N_{0x}$, $\mu_x$, $\Lambda_x$, and $\gamma_x$. The required expressions are tabulated in Table 1.

Based on (54), Table 2 lists the complete set of conversions between parameters of MGDs referenced to $m$, $D_g$, $D_e$, $D_a$, or $A$ as the independent variable. For conversions between PSD representations using radius and diameter, see (51).

## 6. Implications for model fitting

The conversion relationships obtained between different representations of a PSD reveal some potential traps for the unwary when estimating model parameters from real data. To take a simple example, an imaging probe can yield simultaneous estimates of both $A$ and $D_g$ for all of the sampled particles, which in turn can be used to separately obtain (e.g., via moment matching) the four MGD parameters (each) of $n_A(A)$ and $n_g(D_g)$. Values of $\alpha$ and $\beta$ can then be determined in one of at least two ways: 1) by independently estimating these coefficients via a power-law fit to the sample of $A$ and $D_g$, or 2) by solving for $\alpha$ and $\beta$ from the MGD parameters determined separately for $n_A(A)$ and $n_g(D_g)$.

But from the conversions given in Table 2, we see that four model parameters (e.g., $N_{0A}$, $\mu_A$, $\Lambda_A$, and $\gamma_A$) can be computed exactly from the remaining six (e.g., $N_{0g}$, $\mu_g$, $\Lambda_g$, $\gamma_g$, $\alpha$, and $\beta$). In other words, the 10 model parameters that could in principle be directly estimated from particle data collected by an imaging probe are not independent and in fact represent only 6 degrees of freedom. Unless care is taken, one is likely to obtain estimates of the 10 parameters that are not mutually consistent. Indeed, even if one simply computes $\alpha$ and $\beta$ from the other parameters [e.g., $\alpha = (\Lambda_g/\Lambda_A)^{1/\gamma_A}$, $\beta = \gamma_g/\gamma_A$], we are still left with 6 mathematical degrees of freedom among the 8 remaining PSD parameters, which means

TABLE 2. Complete set of conversions between the parameters of MGDs referenced to various particle size descriptors discussed in this paper. Row headings indicate the size descriptor used by the source MGD; column headings indicate the parameters of the target MGD.

| Parameters of target MGD | Size descriptors in source MGD | | | |
|---|---|---|---|---|
| | $N_{0\mathrm{m}}$ | $\mu_m$ | $\Lambda_m$ | $\gamma_m$ |
| $D_g$ | $\frac{1}{b}N_{0g}a^{-(1/b)(\mu_g+1)}$ | $\frac{1}{b}(\mu_g+1)-1$ | $\Lambda_g a^{-\gamma_g/b}$ | $\frac{\gamma_g}{b}$ |
| $D_e$ | $\frac{1}{3}N_{0e}a_0^{-(1/3)(\mu_e+1)}$ | $\frac{1}{3}(\mu_e+1)-1$ | $\Lambda_e a_0^{-\gamma_e/3}$ | $\frac{\gamma_e}{3}$ |
| $D_a$ | $\frac{\beta}{2b}N_{0a}\left(\frac{\alpha}{\alpha_0}\right)^{(1/2)(\mu_a+1)}a^{-(\beta/2b)(\mu_a+1)}$ | $\frac{\beta}{2b}(\mu_a+1)-1$ | $\Lambda_a\left(\frac{\alpha}{\alpha_0}\right)^{\gamma_a/2}a^{-\beta\gamma_a/2b}$ | $\frac{\beta\gamma_a}{2b}$ |
| $A$ | $\frac{\beta}{b}N_{0A}a^{-(\beta/b)(\mu_A+1)}\alpha^{\mu_A+1}$ | $\frac{\beta}{b}(\mu_A+1)-1$ | $\Lambda_A\alpha^{\gamma_A}a^{-\beta\gamma_A/b}$ | $\frac{\beta\gamma_A}{b}$ |
| | $N_{0\mathrm{g}}$ | $\mu_g$ | $\Lambda_g$ | $\gamma_g$ |
| $m$ | $bN_{0m}a^{\mu_m+1}$ | $b(\mu_m+1)-1$ | $\Lambda_m a^{\gamma_m}$ | $b\gamma_m$ |
| $D_e$ | $\frac{b}{3}N_{0e}\left(\frac{a}{a_0}\right)^{(1/3)(\mu_e+1)}$ | $\frac{b}{3}(\mu_e+1)-1$ | $\Lambda_e\left(\frac{a}{a_0}\right)^{\gamma_e/3}$ | $\frac{b\gamma_e}{3}$ |
| $D_a$ | $\frac{\beta}{2}N_{0a}\left(\frac{\alpha}{\alpha_0}\right)^{(1/2)(\mu_a+1)}$ | $\frac{\beta}{2}(\mu_a+1)-1$ | $\Lambda_a\left(\frac{\alpha}{\alpha_0}\right)^{\gamma_a/2}$ | $\frac{\beta\gamma_a}{2}$ |
| $A$ | $\beta N_{0A}\alpha^{\mu_A+1}$ | $\beta(\mu_A+1)-1$ | $\Lambda_A\alpha^{\gamma_A}$ | $\beta\gamma_A$ |
| | $N_{0e}$ | $\mu_e$ | $\Lambda_e$ | $\gamma_e$ |
| $m$ | $3N_{0m}a_0^{\mu_m+1}$ | $3(\mu_m+1)-1$ | $\Lambda_m a_0^{\gamma_m}$ | $3\gamma_m$ |
| $D_g$ | $\frac{3}{b}N_{0g}\left(\frac{a_0}{a}\right)^{(1/b)(\mu_g+1)}$ | $\frac{3}{b}(\mu_g+1)-1$ | $\Lambda_g\left(\frac{a_0}{a}\right)^{\gamma_g/b}$ | $\frac{3\gamma_g}{b}$ |
| $D_a$ | $\frac{3\beta}{2b}N_{0a}\left(\frac{a_0}{a}\right)^{(\beta/2b)(\mu_a+1)}\left(\frac{\alpha}{\alpha_0}\right)^{(1/2)(\mu_a+1)}$ | $\frac{3\beta}{2b}(\mu_a+1)-1$ | $\Lambda_a\left(\frac{a_0}{a}\right)^{\beta\gamma_a/2b}\left(\frac{\alpha}{\alpha_0}\right)^{\gamma_a/2}$ | $\frac{3\beta\gamma_a}{2b}$ |
| $A$ | $\frac{3\beta}{b}N_{0A}\alpha^{\mu_A+1}\left(\frac{a_0}{a}\right)^{(\beta/b)(\mu_A+1)}$ | $\frac{3\beta}{b}(\mu_A+1)-1$ | $\Lambda_A\alpha^{\gamma_A}\left(\frac{a_0}{a}\right)^{\beta\gamma_A/b}$ | $\frac{3\beta\gamma_A}{b}$ |
| | $N_{0a}$ | $\mu_a$ | $\Lambda_a$ | $\gamma_a$ |
| $m$ | $\frac{2b}{\beta}N_{0m}a^{\mu_m+1}\left(\frac{\alpha_0}{\alpha}\right)^{(b/\beta)(\mu_m+1)}$ | $\frac{2b}{\beta}(\mu_m+1)-1$ | $\Lambda_m a^{\gamma_m}\left(\frac{\alpha_0}{\alpha}\right)^{b\gamma_m/\beta}$ | $\frac{2b\gamma_m}{\beta}$ |
| $D_g$ | $\frac{2}{\beta}N_{0g}\left(\frac{\alpha_0}{\alpha}\right)^{(1/\beta)(\mu_g+1)}$ | $\frac{2}{\beta}(\mu_g+1)-1$ | $\Lambda_g\left(\frac{\alpha_0}{\alpha}\right)^{\gamma_g/\beta}$ | $\frac{2\gamma_g}{\beta}$ |
| $D_e$ | $\frac{2b}{3\beta}N_{0e}\left(\frac{a}{a_0}\right)^{(1/3)(\mu_e+1)}\left(\frac{\alpha_0}{\alpha}\right)^{(b/3\beta)(\mu_e+1)}$ | $\frac{2b}{3\beta}(\mu_e+1)-1$ | $\Lambda_e\left(\frac{a}{a_0}\right)^{\gamma_e/3}\left(\frac{\alpha_0}{\alpha}\right)^{b\gamma_e/3\beta}$ | $\frac{2b\gamma_e}{3\beta}$ |
| $A$ | $2N_{0A}\alpha_0^{\mu_A+1}$ | $2(\mu_A+1)-1$ | $\Lambda_A\alpha_0^{\gamma_A}$ | $2\gamma_A$ |
| | $N_{0A}$ | $\mu_A$ | $\Lambda_A$ | $\gamma_A$ |
| $m$ | $\frac{b}{\beta}N_{0m}a^{\mu_m+1}\alpha^{-(b/\beta)(\mu_m+1)}$ | $\frac{b}{\beta}(\mu_m+1)-1$ | $\Lambda_m a^{\gamma_m}\alpha^{-b\gamma_m/\beta}$ | $\frac{b\gamma_m}{\beta}$ |
| $D_g$ | $\frac{1}{\beta}N_{0g}\alpha^{-(1/\beta)(\mu_g+1)}$ | $\frac{1}{\beta}(\mu_g+1)-1$ | $\Lambda_g\alpha^{-\gamma_g/\beta}$ | $\frac{\gamma_g}{\beta}$ |
| $D_e$ | $\frac{b}{3\beta}N_{0e}\alpha^{-(b/3\beta)(\mu_e+1)}\left(\frac{a}{a_0}\right)^{(1/3)(\mu_e+1)}$ | $\frac{b}{3\beta}(\mu_e+1)-1$ | $\Lambda_e\left(\frac{a}{a_0}\right)^{\gamma_e/3}\alpha^{-b\gamma_e/3\beta}$ | $\frac{b\gamma_e}{3\beta}$ |
| $D_a$ | $\frac{1}{2}N_{0a}\alpha_0^{-(1/2)(\mu_a+1)}$ | $\frac{1}{2}(\mu_a+1)-1$ | $\Lambda_a\alpha_0^{-\gamma_a/2}$ | $\frac{\gamma_a}{2}$ |

that separate curve or moment fits to noisy data will likely lead to mathematical inconsistencies. An interesting question (and one not answered here) is what procedures exist, or could be devised, to optimally derive all 10 parameters from a set of simultaneous observations of both $A$ and $D_g$ while enforcing perfect mathematical self-consistency. Another question is whether the resulting fits would also be more robust in other measurable ways.

## 7. Rescaled size distribution

A fairly recent innovation is the use of normalizing or rescaling procedures to obtain a nondimensional PSD expressed as a function of a nondimensional size defined in terms of the actual geometric size and various moments of the original PSD (Testud et al. 2001; Lee et al. 2004; Westbrook et al. 2004; Delanoë et al. 2005; F07; Tian et al. 2010). One motivation is to "explore the underlying shape of the PSD without imposing any a priori expectation for any specific analytic form" (F07). Another is to capture (or parameterize) a spectrum of PSDs in terms of one or two reasonably generic properties such as the low-order moments of the distribution.

To give one example, F07 employ a two-moment rescaling of snow PSDs as follows:

$$\Phi_{23}(x) = n_g(D_g)\frac{M_3^3}{M_2^4}, \quad x = D_g\frac{M_2}{M_3}, \tag{55}$$

where $M_k$ is the $k$th moment of the PSD, $x$ is a nondimensional particle size, and $\Phi_{23}(x)$ is the nondimensional size distribution obtained used the second and third moments.

It is instructive to apply the above rescaling procedure to the MGD using the analytic expressions for the moments given in (17):

$$x = D_g\Lambda_g^{1/\gamma_g}\frac{\Gamma\left(\frac{\mu_g+3}{\gamma_g}\right)}{\Gamma\left(\frac{\mu_g+4}{\gamma_g}\right)}, \tag{56}$$

$$\Phi_{23}(x) = N_{0x}x^{\mu_x}\exp(-\Lambda_x x^{\gamma_x}), \tag{57}$$

where

$$N_{0x} = \frac{\gamma_g}{\Gamma\left(\frac{\mu_g+3}{\gamma_g}\right)}\left[\frac{\Gamma\left(\frac{\mu_g+4}{\gamma_g}\right)}{\Gamma\left(\frac{\mu_g+3}{\gamma_g}\right)}\right]^{\mu_g+3},$$

$$\mu_x = \mu_g,$$

$$\gamma_x = \gamma_g, \quad \text{and}$$

$$\Lambda_x = \frac{\Gamma\left(\frac{\mu_g+4}{\gamma_g}\right)}{\Gamma\left(\frac{\mu_g+3}{\gamma_g}\right)}. \tag{58}$$

The rescaled MGD is thus another MGD, but the four parameters of the rescaled MGD depend on only two parameters of the original MGD: $\mu_g$ and $\gamma_g$. The parameters $N_{0g}$ and $\Lambda_g$ play no role in the rescaled MGD, the second of these parameters having been absorbed into the definition of $x$. Moreover, the parameters $\mu$ and $\gamma$ are unchanged by the rescaling. It follows that any pure exponential PSD ($\mu = 0$, $\gamma = 1$) rescales to the fixed form (F07):

$$\Phi_{23}(x) = \frac{27}{2}\exp(-3x). \tag{59}$$

Because the values of two parameters of the original MGD are lost in the rescaling, its reconstruction from $\Phi_{23}(x)$ requires the additional specification of any two independent properties (e.g., moments) of the original PSD.

## 8. Example applications

A major purpose for deriving conversions between various equivalent representations of PSDs is to facilitate convenient and direct comparison of PSDs from different sources regardless of the manner in which they were originally specified. Here we consider three published PSDs for snow particles:

(i) a representative measured PSD from Braham (1990, hereafter B90) expressed in terms of $D_g$ of the snowflakes observed in lake effect snow;
(ii) the snow PSD of SS70, which is a function of liquid-equivalent precipitation rate $R$ and expressed in terms of liquid-equivalent diameter $D_e$; and
(iii) the PSD obtained for "snow" in midlatitude stratiform ice cloud by F07, which is given in the nondimensional (rescaled) form described in the previous section and with $x$ as the independent variable.

Note that the snow observed at altitude by F07 is from a markedly different environment than the near-surface snowfall measured by B90 and SS70, and we can therefore expect, a priori, that the three PSDs will not be similar. Our premise, however, is that the PSDs cannot be compared even qualitatively until recast into a common framework.

For the sake of the present illustration, and following F07, we assume the snow particle mass–size relationship of Wilson and Ballard (1999) [$a = 0.069$ and $b = 2.0$ in (29)], which is fairly typical of empirically derived relationships in showing an approximate $D^2$ dependence of particle mass on geometric diameter. The precise relationship used here is unimportant, since our focus is on the methods and not on the quantitative results.

To be comparable, we require all three PSDs to yield identical snow/ice water content $W$. While SS70 and F07 are parametric and can be varied to yield arbitrary values of $W$, B90 give a series of exponential fits to discrete observations of PSDs in lake effect snow. We therefore choose one representative example from B90 and adjust the other two PSDs to match. Details are given below.

### *a. B90*

Table 4 of B90 gives fitted parameters for 49 observed snow spectra, assuming an exponential distribution of the form

TABLE 3. MGD coefficients (SI units) for three published snow PSDs (see text), all yielding a snow water content of 0.306 g m$^{-3}$.

| PSD | $N_{0e}$ | $\mu_e$ | $\Lambda_e$ | $\gamma_e$ | $N_{0g}$ | $\mu_g$ | $\Lambda_g$ | $\gamma_g$ |
|---|---|---|---|---|---|---|---|---|
| B90 | $9.394 \times 10^8$ | 0.5 | $1.289 \times 10^5$ | 1.5 | $7.19 \times 10^6$ | 0 | 1480 | 1 |
| SS70 | $2.317 \times 10^6$ | 0 | 2208 | 1 | $7.861 \times 10^4$ | −0.333 | 112.4 | 0.667 |
| F07 (1) | $7.355 \times 10^{10}$ | 0.5 | $1.411 \times 10^6$ | 1.5 | $5.629 \times 10^8$ | 0 | $1.62 \times 10^4$ | 1 |
| F07 (2) | $8.304 \times 10^{20}$ | 3.605 | $4.049 \times 10^5$ | 1.5 | $6.126 \times 10^{14}$ | 2.07 | 4648 | 1 |

$$n_g(D_g) = N_{0g} \exp(-\Lambda_g D_g). \tag{60}$$

We arbitrarily chose their 1030 EST 19 December 1983 distribution (19D1030) as representative of moderately high snow water content. For this case,

$$N_{0g} = 7.19 \times 10^6 \text{ m}^{-4}, \quad \Lambda_g = 1480 \text{ m}^{-1}. \tag{61}$$

B90 integrated this PSD assuming a spherical shape and a constant bulk density of 0.025 g cm$^{-3}$ to obtain a snow water content of 0.118 g m$^{-3}$. We integrated it using $m = aD_g^b$ to obtain a much higher $W = 0.306$ g m$^{-3}$. While the (unknowable) true snow water content for this case is not pertinent to the present illustration, the divergence between these two estimates of $W$ underscores the sensitivity of snow water calculations to particle density assumptions.

### b. SS70

The snow PSD of SS70 is given by

$$n_e(D_e) = N_{0e} \exp(-\Lambda_e D_e), \tag{62}$$

where

$$N_{0e} = 2.50 \times 10^3 R^{-0.94} \,(\text{mm}^{-1}\ \text{m}^{-3}) \quad \Lambda_e = 22.9 R^{-0.45} \,(\text{cm}^{-1}) \tag{63}$$

and $R$ is in millimeters per hour. We adjusted $R$ until we reproduced the snow water content of 0.306 g m$^{-3}$ found previously for B90, yielding $R = 1.084$ mm h$^{-1}$ and

$$N_{0e} = 2.317 \times 10^6 \text{ m}^{-4}, \quad \Lambda_e = 2208 \text{ m}^{-1}. \tag{64}$$

### c. F07

F07 give the following normalized form for the PSD of particles observed in midlatitude stratiform ice clouds:

$$\Phi_{23}(x) = 141 \exp(-16.8x) + 102x^{2.07} \exp(-4.82x). \tag{65}$$

In other words, it is a sum of exponential and gamma distributions expressed in terms of $x$ defined in (55).

As noted earlier, it is necessary to specify two moments in order to recover the original PSD. However, F07 also present an empirical relationship between moments of their distributions, so that the specification of a single moment is sufficient to uniquely determine all moments of the PSD. The second and third moments are thus related by the equations given in their Table 3, and the second moment $M_2$ in particular is proportional to snow water content by virtue of the assumed $D^2$ dependence of particle mass. Assuming a temperature of −10°C, we find that $M_2 = 0.004\,452$ (SI units) yields the target snow water content of 0.306 g m$^{-3}$, so that

$$n_g(D_g) = N_{0g1} \exp(-\Lambda_{g1} D_g) + N_{0g2} D_g^{\mu_{g2}} \exp(-\Lambda_{g2} D_g), \tag{66}$$

where (in SI units)

$$N_{0g1} = 5.629 \times 10^8, \quad \Lambda_{g1} = 1.62 \times 10^4, \quad N_{0g2} = 6.126 \times 10^{14}, \quad \mu_{g2} = 2.07, \quad \Lambda_{g2} = 4.648 \times 10^3. \tag{67}$$

### d. Conversions

For the above three PSDs, the parameters $\mu = 0$ and $\gamma = 0$ unless otherwise noted. With all four parameters of the MGD specified for a given published distribution (or, in the case of F07, for each term in the composite distribution), we can apply the appropriate conversions in Table 2 to find alternate representations in terms of $D_g$ or $D_e$. The parameter values for these alternate forms are given in Table 3.

Note that as a consequence of assuming $b < 3$ in (29), both B90 and F07 translate into MGDs when expressed as $n_e(D_e)$, and SS70 becomes an MGD when expressed as $n_g(D_g)$.

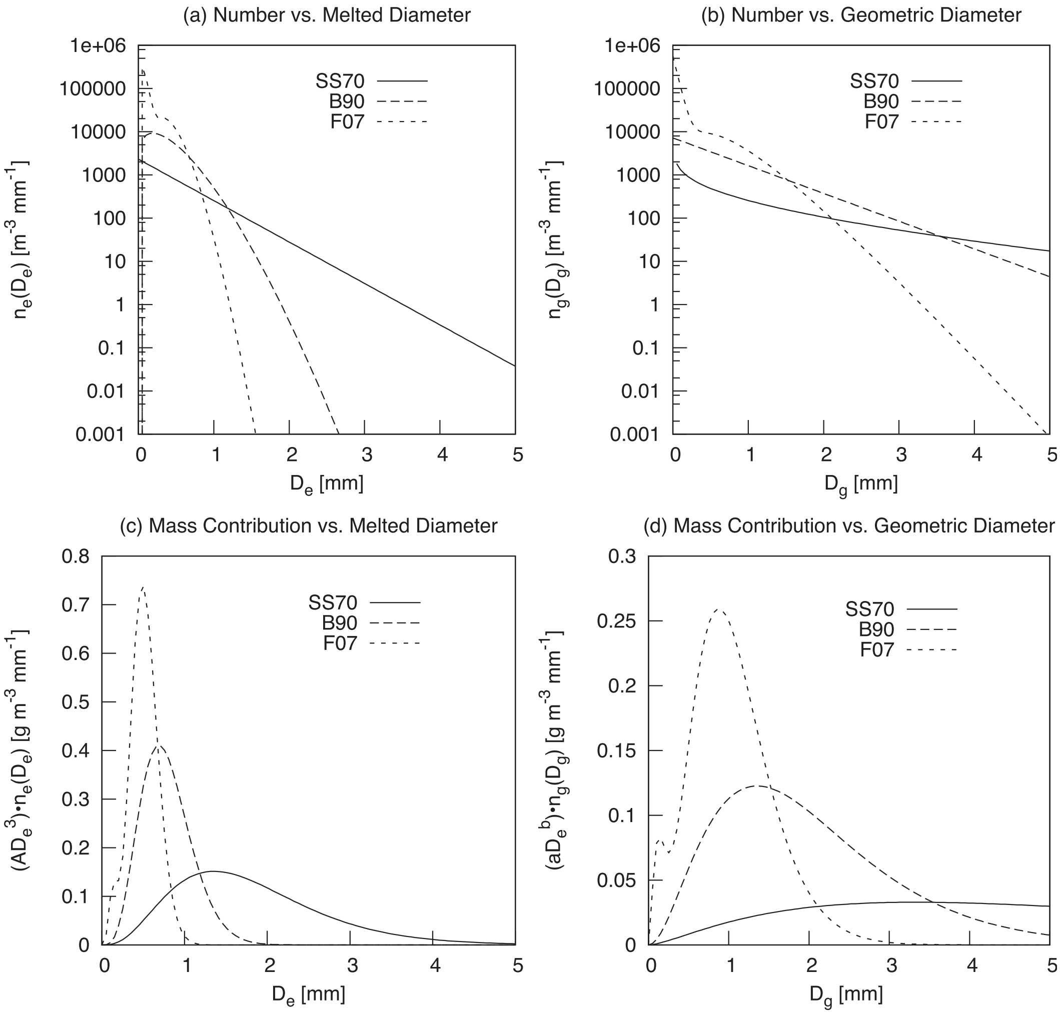


FIG. 1. Three example snow PSDs, each with parameters chosen so as to integrate to the same total snow water content of 0.306 g $m^{-3}$: SS70 (solid), B90 (long dashed), and the midlatitude PSD of F07 (short dashed). PSDs are presented as number concentrations per unit (a) $D_e$ and (b) $D_g$, and as mass contributions per unit (c) $D_e$ and (d) $D_g$. Conversions between $D_g$ and $D_e$ assume the mass–diameter relationship $M = 0.069D_g^2$ (SI units).

### *e. Comparisons*

Recalling that all three PSDs described above yield the same snow/ice water content, they may now be directly compared by plotting the appropriate forms as functions of $D_e$ (Fig. 1, left column) or $D_g$ (right column). The differences between the three distributions are striking. In terms of both number concentration (top row) and mass contribution (bottom row), the SS70 distribution is notable for yielding numerous large particles greatly exceeding 2 mm in melted diameter and 4 mm in geometric diameter. These dimensions are consistent with fairly large snow aggregates. At the other extreme, the F07 distribution yields very few particles larger than 1-mm melted diameter or 2-mm geometric diameter.

The shapes of the PSDs are also distinct, with SS70 being concave-upward in Fig. 1b, while F07 is concave-downward over most of the range. The F07 distribution expressed as mass contribution versus $D_g$ (Fig. 1d) is also notable for have a second mode at small sizes. In terms of both size and shape, B90 falls between SS70 and F07.

The corresponding median mass melted diameters are 0.503 (F07; determined numerically), 0.755 (B90), and 1.67 mm (SS70), more than a factor of 3 range for the same snow water content. A back-of-the-envelope calculation of equivalent radar reflectivity factors using the sixth moment of the distributions (i.e., assuming the validity of the Rayleigh approximation applied to the volume-equivalent diameters) yields results ranging from 13.6 d$BZ_e$ for F07 to 31.6 d$BZ_e$ for SS70, an 18-d$BZ$ difference.

That the above differences are significant is not unexpected in view of the very different conditions under which the PSDs were obtained. The major point relevant to this paper is that these PSDs *could* be directly compared in multiple frameworks with so little effort, once the necessary conversions had been derived and tabulated in Table 2 along with the analytic expression for the moments given in (17).

## 9. Conclusions

Our review and mathematical analysis of the general PSD model known as the modified gamma distribution highlights the fundamental relevance of the MGD when working with nonspherical atmospheric particles whose area and mass scale with $\alpha D_g^\beta$ and $D_g^b$, respectively, especially when $b < 3$. In particular, a PSD that is a pure exponential or three-parameter gamma distribution when referenced to one size descriptor almost inevitably becomes a four-parameter MGD when referenced to another.

Our findings are consistent with Auf der Maur (2001) but we provide, in Table 2, explicit and convenient rules for the conversion between MGDs expressed in terms of a variety of size representations, including geometric diameter $D_g$, volume-equivalent diameter $D_e$, area-equivalent diameter $D_a$, mass $m$, and surface or projected area $A$.

By way of illustration, we employed our conversions to transform three published PSDs for "snow"—those of SS70, B90, and F07—into common frames of reference. While large differences in these PSDs were expected owing to differences in the methods and circumstances of the data collection, our conversion of the PSDs to common bases made it straightforward to compare them in more quantitative terms, confirming that the dissimilarities are quite large—a factor of 3 difference in median mass diameter and a roughly 18-dB$Z$ difference in radar reflectivity for the same snow/ice water content of 0.306 g m$^{-3}$. We emphasize that the specific results of these comparisons are tied to both the mass–size relationship used and to the fixed snow water content assumed. Our focus here is on the methods and on the central role of the MGD, not on the quantitative results for specific published PSD models.

The tabulated relationships given herein are intended not only for the purpose of comparisons like the above, but also to facilitate routine work with the MGD family of particle size distribution models, including common exponential and gamma distributions as size descriptor-dependent special cases.

*Acknowledgments.* This work was supported by NASA Grants NNX07AE29G and NNX10AGAH69G in support of the Precipitation Measurement Mission (PMM). We thank Dr. Mark Kulie for helpful discussions and two anonymous reviewers for suggestions that led to major improvements to the paper.

REFERENCES

Ackerman, S. A., and G. L. Stephens, 1987: The absorption of solar radiation by cloud droplets: An application of anomalous diffraction theory. *J. Atmos. Sci.,* **44,** 1574–1588.

Auf der Maur, A. N., 2001: Statistical tools for drop size distributions: Moments and generalized gamma. *J. Atmos. Sci.,* **58,** 407–418.

Babb, D. M., J. Verlinde, and B. A. Albrecht, 1999: Retrieval of cloud microphysical parameters from 94-GHz radar Doppler power spectra. *J. Atmos. Oceanic Technol.,* **16,** 489–503.

Braham R. R., Jr., 1990: Snow particle size spectra in lake effect snows. *J. Appl. Meteor.,* **29,** 200–207.

Brandes, E., K. Ikeda, G. Zhand, M. Schönhuber, and R. M. Rasmussen, 2007: A statistical and physical description of hydrometeor distributions in Colorado snowstorms using a video disdrometer. *J. Appl. Meteor. Climatol.,* **46,** 634–650.

Brawn, D., and G. Upton, 2007: Closed-form parameter estimates for a truncated gamma distribution. *Environmetrics,* **18,** 633–645.

Brown, P. R. A., and P. N. Francis, 1995: Improved measurements of the ice water content in cirrus using a total-water probe. *J. Atmos. Oceanic Technol.,* **12,** 410–414.

Deirmendjian, D., 1963: Scattering and polarization properties of polydispersed suspensions with partial absorption. *Electromagnetic Scattering,* M. Kerker, Ed., Pergamon Press, 171–189.

——, 1969: *Electromagnetic Scattering on Spherical Polydispersions*. Elsevier, 290 pp.

Delanoë, J., A. Protat, J. Testud, D. Bouniol, A. J. Heymsfield, A. Bansemer, P. R. A. Brown, and R. M. Forbes, 2005: Statistical properties of the normalized ice particle size distribution. *J. Geophys. Res.,* **110,** D10201, doi:10.1029/2004JD005405.

——, ——, D. Bouniol, A. Heymsfield, A. Bansemer, and P. Brown, 2007: The characterization of ice cloud properties from Doppler radar measurements. *J. Appl. Meteor. Climatol.,* **46,** 1682–1698.

Field, P., A. Heymsfield, and A. Bansemer, 2007: Snow size distribution parameterization for midlatitude and tropical ice clouds. *J. Atmos. Sci.,* **64,** 4346–4365.

Grecu, M., W. S. Olson, and E. N. Anagnostou, 2004: Retrieval of precipitation profiles from multiresolution, multifrequency active and passive microwave observations. *J. Appl. Meteor.,* **43,** 562–575.

Gunn, K. L. S., and J. S. Marshall, 1958: The distribution with size of aggregate snowflakes. *J. Atmos. Sci.,* **15,** 452–461.

Hansen, J. E., and L. D. Travis, 1974: Light scattering in planetary atmospheres. *Space Sci. Rev.,* **16,** 527–610.

Hess, M., P. Koepke, and I. Schult, 1998: Optical properties of aerosols and clouds: The software package OPAC. *Bull. Amer. Meteor. Soc.,* **79,** 831–844.

Heymsfield, A. J., and L. M. Miloshevich, 2003: Parameterizations for the cross-sectional area and extinction of cirrus and stratiform ice cloud particles. *J. Atmos. Sci.,* **60,** 936–956.

——, A. Bansemer, P. R. Field, S. L. Durden, J. Stith, J. Dye, W. Hall, and C. Grainger, 2002: Observations and parameterizations of particle size distributions in deep tropical cirrus and stratiform precipitating clouds: Results from in situ observations in TRMM field campaigns. *J. Atmos. Sci.,* **59,** 3457–3491.

——, ——, C. Schmitt, C. Twohy, and M. Poellot, 2004: Effective ice particle densities derived from aircraft data. *J. Atmos. Sci.,* **61,** 982–1003.

——, C. G. Schmitt, A. Bansemer, and C. H. Twohy, 2010: Improved representation of ice particle masses based on observations in natural clouds. *J. Atmos. Sci.,* **67,** 3303–3318.

Iguchi, T., T. Kozu, R. Meneghini, J. Awaka, and K. Okamoto, 2000: Rain-profiling algorithm for the TRMM Precipitation Radar. *J. Appl. Meteor.,* **39,** 2038–2051.

Jameson, A., 1993: Estimating the path-average rainwater content and updraft speed along a microwave link. *J. Atmos. Oceanic Technol.,* **10,** 478–485.

Junge, C., 1955: The size distribution and aging of natural aerosols as determined from electrical and optical data on the atmosphere. *J. Meteor.,* **12,** 13–25.

Kozu, T., and K. Nakamura, 1991: Rainfall parameter estimation from dual-radar measurements combining reflectivity profile and path-integrated attenuation. *J. Atmos. Oceanic Technol.,* **8,** 259–270.

Kuo, K., E. A. Smith, Z. Haddad, E. Im, T. Iguchi, and A. Mugnai, 2004: Mathematical–physical framework for retrieval of rain DSD properties from dual-frequency Ku–Ka-band satellite radar. *J. Atmos. Sci.,* **61,** 2349–2369.

Lee, G., I. Zawadzki, W. Szyrmer, D. Sempere-Torres, and R. Uijlenhoet, 2004: A general approach to double-moment normalization of drop size distributions. *J. Appl. Meteor.,* **43,** 264–281.

Locatelli, J. D., and P. V. Hobbs, 1974: Fall speeds and masses of solid precipitation particles. *J. Geophys. Res.,* **79,** 2185–2197.

Maki, M., T. D. Keenan, Y. Sasaki, and K. Nakamura, 2001: Characteristics of the raindrop size distribution in tropical continental squall lines observed in Darwin, Australia. *J. Appl. Meteor.,* **40,** 1393–1412.

Mallet, C., and L. Barthes, 2009: Estimation of gamma raindrop size distribution parameters: Statistical fluctuations and estimation errors. *J. Atmos. Oceanic Technol.,* **26,** 1572–1584.

Marshall, J. S., and W. H. Palmer, 1948: The distribution of raindrops with size. *J. Meteor.,* **5,** 165–166.

McFarquhar, G. M., and A. J. Heymsfield, 1998: The definition and significance of an effective radius for ice clouds. *J. Atmos. Sci.,* **55,** 2039–2052.

Meneghini, R., T. Kozu, H. Kumagai, and W. Boncyk, 1992: A study of rain estimation methods from space using dual-wavelength radar measurements at near-nadir incidence over ocean. *J. Atmos. Oceanic Technol.,* **9,** 364–382.

Miles, N. L., J. Verlinde, and E. E. Clothiaux, 2000: Cloud droplet size distributions in low-level stratiform clouds. *J. Atmos. Sci.,* **57,** 295–311.

Mitchell, D. L., 1991: Evolution of snow-size spectra in cyclonic storms. Part II: Deviations from the exponential form. *J. Atmos. Sci.,* **48,** 1885–1899.

——, 1996: Use of mass- and area-dimensional power laws for determining precipitation particle terminal velocities. *J. Atmos. Sci.,* **53,** 1710–1723.

——, 2002: Effective diameter in radiative transfer: General definition, applications, and limitations. *J. Atmos. Sci.,* **59,** 2330–2346.

——, and W. P. Arnott, 1994: A model predicting the evolution of ice particle size spectra and radiative properties of cirrus clouds. Part II: Dependence of absorption and extinction on ice crystal morphology. *J. Atmos. Sci.,* **51,** 817–832.

——, and A. J. Heymsfield, 2005: Refinements in the treatment of ice particle terminal velocities, highlighting aggregates. *J. Atmos. Sci.,* **62,** 1637–1644.

——, A. Macke, and Y. Liu, 1996: Modeling cirrus clouds. Part II: Treatment of radiative properties. *J. Atmos. Sci.,* **53,** 2967–2988.

Muller, B. M., H. E. Fuelberg, and E. A. Smith, 1993: An alternative representation of the ice canopy for calculating microwave brightness temperatures over a thunderstorm. *J. Appl. Meteor.,* **32,** 1006–1013.

Petty, G. W., and W. Huang, 2010: Microwave backscatter and extinction by soft ice spheres and complex snow aggregates. *J. Atmos. Sci.,* **67,** 769–787.

Rose, C., and V. Chandrasekar, 2006: A GPM dual-frequency retrieval algorithm: DSD profile-optimization method. *J. Atmos. Oceanic Technol.,* **23,** 1372–1383.

Schmitt, C. G., and A. J. Heymsfield, 2009: The size distribution and mass-weighted terminal velocity of low-latitude tropopause cirrus crystal populations. *J. Atmos. Sci.,* **66,** 2013–2028.

——, and ——, 2010: The dimensional characteristics of ice crystal aggregates from fractal geometry. *J. Atmos. Sci.,* **67,** 1605–1616.

Schneider, T. L., and G. L. Stephens, 1995: Theoretical aspects of modeling backscattering by cirrus ice particles at millimeter wavelengths. *J. Atmos. Sci.,* **52,** 4367–4385.

Sekhon, R. S., and R. C. Srivastava, 1970: Snow size spectra and radar reflectivity. *J. Atmos. Sci.,* **27,** 299–307.

Smith, P., and D. Kliche, 2005: The bias in moment estimators for parameters of drop size distribution functions: Sampling from exponential distributions. *J. Appl. Meteor.,* **44,** 1195–1205.

Straka, J. M., 2009: *Cloud and Precipitation Microphysics: Principles and Parameterizations*. Cambridge University Press, 392 pp.

Sun, X., Y. Han, and H. Wang, 2006: Near-infrared light scattering by ice-water mixed clouds. *Prog. Electromag. Res.,* **61,** 133–142.

Testud, J., S. Oury, R. A. Black, P. Amayenc, and X. Dou, 2001: The concept of ''normalized'' distribution to describe raindrop spectra. A tool for cloud physics and cloud remote sensing. *J. Appl. Meteor.,* **40,** 1118–1140.

Tian, L., G. M. Heymsfield, A. J. Heymsfield, A. Bansemer, L. Li, C. H. Twohy, and R. C. Srivastava, 2010: A study of cirrus ice particle size distribution using TC4 observations. *J. Atmos. Sci.,* **67,** 195–216.

Tomasi, C., R. Guzzi, and O. Vittori, 1975: The ''$SO_2$–$NH_3$—solution droplets'' system in an urban atmosphere. *J. Atmos. Sci.,* **32,** 1580–1586.

Ulbrich, C. W., 1983: Natural variations in the analytical form of the raindrop size distribution. *J. Climate Appl. Meteor.,* **22,** 1764–1775.

——, 1985: The effects of drop size distribution truncation on rainfall integral parameters and empirical relations. *J. Climate Appl. Meteor.,* **24,** 580–590.

Vivekanandan, J., B. E. Martner, M. K. Politovich, and G. Zhang, 1999: Retrieval of atmospheric liquid and ice characteristic using dual-wavelength radar observations. *IEEE Trans. Geosci. Remote Sens.,* **37,** 2325–2334.

Westbrook, C. D., R. C. Ball, P. R. Field, and A. J. Heymsfield, 2004: Theory of growth by differential sedimentation, with application to snowflake formation. *Phys. Rev. E,* **70,** 021403, doi:10.1103/PhysRevE.70.021403.

Wilson, D. R., and S. P. Ballard, 1999: A microphysically based precipitation scheme for the UK Meteorological Office Unified Model. *Quart. J. Roy. Meteor. Soc.,* **125,** 1607–1636.